Proceedings of the 21st ICSMGE, Vienna, Austria, 14 – 19 June 2026. Pistrol, Adam & Schweiger (eds.)
Published by: ÖGG, Austrian Society for Geomechanics, Salzburg, Austria, ISBN 978-3-9503898-4-5
https://doi.org/10.53243/ICSMGE2026-1236

Application of pressure surges as a resource-saving soil improvement technique for liquefaction mitigation

Florian Thurner, Roman Marte
Institute of Soil Mechanics, Foundation Engineering and Computational Geotechnics, Graz University of Technology, florian.thurner@tugraz.at

ABSTRACT: Saturated layers of loose soils, primarily sands with a minor content of silt, are critical subsoil conditions with respect to their susceptibility to liquefaction under dynamic loads such as seismic events. Liquefaction occurs when pore water pressure rises, reducing effective stress to zero, causing soil strength loss and liquid-like behavior until the excess pressure dissipates. Existing mitigation methods include strength enhancement (e.g., grouting), an increase in permeability (drainage), and densification. However, these conventional techniques often rely on raw materials and heavy machinery, leading to high costs and significant CO_2 emissions. This highlights the need for innovative, resource-efficient solutions for liquefaction mitigation. This paper introduces a novel soil improvement technique that achieves densification by dynamically applying pressure surges to the water. By leveraging in situ groundwater conditions as a central component of the soil improvement process, the reliance on raw materials can be significantly reduced, resulting in a more environmentally sustainable approach. Experimental results of a small-scale test box are presented, using various measurement devices to analyze the soil's response during and after the applied impulses. The test results clearly demonstrate a densification of the soil layer and lay the groundwork for the current development of a practical system for field applications.

KEYWORDS: liquefaction mitigation, soil improvement, sustainable geotechnics.

1 INTRODUCTION

Soil liquefaction faces a major hazard for infrastructure, buildings, and subsequently also human life, in case of e.g., seismic events. Earthquakes can lead to cyclic liquefaction depending mainly on the local subsoil conditions and the magnitude. Certain ground conditions, mainly sandy soils with a minor content of silt in a very loose to loose and fully saturated state, are prone to cyclic liquefaction (Huang and Yu, 2013). Disasters like the 2011 Tohoku Oki (Japan) and the 2010-2011 Christchurch earthquakes (New Zealand) are recent examples of such earthquake induced liquefaction disasters (EILD) (Pecker 2021; Kramer and Stewart 2025).

Due to the propagation of shear waves, excess pore pressure develops which reduces the effective stresses. If these excess pore pressures reach the same magnitude as the effective stresses, the grain-to-grain-contact gets lost and the soil starts to behave like liquid until the pore pressure decreases again and the soil particles rearrange. (Jefferies and Been 2016)

Current state-of-the-art methods offer a variety of different mitigation techniques, which according to Mitchell (2012, c2008) can be categorized into drainage, void filling, densification (with and without drainage or reinforcement), columns of cemented soil and remove- or replacement. Due to the high CO_2 emissions caused by the usage of raw materials like cement in combination with heavy machinery, recent developments focus on alternative mitigation methods. Bao et al. (2019) and Huang and Wen (2015) highlight, that current research focuses on new concepts like microbiological geotechnology, passive site remediation and induced partial saturation, using for e.g. nanomaterials, short synthetic fibers and biological materials. As a lot of these materials are still in the lab test phase, their applicability in field has yet to be verified.

While recent research works towards the application of new materials, less focus is put on new technical solutions. In this paper, a novel liquefaction mitigation technique, called Dynamic Water Impulse Compaction (DYWIC), is presented, using only the in situ ground water as a densification medium. Through the application of pressure surges over a pipe filled with water, which is perforated and thus in contact with the surrounding soil inside the layer of interest, a rearrangement of the soil into a denser state is targeted. These surges increase the pore pressure to a level matching the effective stresses, inducing localized liquefaction. Consequently, the soil behaves like a liquid until the excess pore pressure dissipates, allowing the particles to rearrange into a denser state.

Multiple small-scale tests have been performed to investigate the basic principle of operation and the behavior of the soil under the pressure surges and evaluate the effectiveness under laboratory conditions. The paper explains the setup and the measurement devices used for the tests, presents selected results, discusses the effects occurring in the soil and give recommendations for further laboratory and field tests.

2 METHODOLOGY

2.1 *General*

Increasing the pore pressure by only targeting the water in the fully saturated voids of the soil is a different approach on achieving soil liquefaction compared to what is usually caused by shearing (e.g. earthquakes, vibro compaction). However, the effect of temporarily bringing the soil into a state of liquid-like behaviour followed by a densification is a shared interest of existing methods and the here presented novel one. The literature does not offer much valuable information about the processes taking place in the soil, if only the pore pressure is raised dynamically without an antecedent shearing as most publications in this field are dealing with earthquake induced liquefaction. In order to gain a better understanding of the mechanisms during repeatedly applied pressure surges, a series of laboratory test have been performed. The setup of the test box was similar for all tests; therefore, one representative setup, execution and results are shown in this paper.

2.2 *Test box specifications*

The test box' inner dimensions, depicted in Figure 1, measure 76/46/56 cm, whereas the coordinate system for the result plots discussed in chapter 3 is located at the bottom of the box in the centre of the axis of symmetry (see Figure 1). In total, 250 kg of sand and 84 litres of water were installed. The water level is located at Z = app. 40 cm and the surface of the sand lies at Z = app. 50 cm, as shown in Figure 2. During the installation of the soil above the water level, the expected suction effects of the sand, which led to partial saturation, were counteracted by adding water inside the perforated pipe to maintain a constant

water level. The soil used for the laboratory tests was chosen based on literature, suggesting a span of grain size distribution for soils suspectable to liquefaction (Laue and Buchheister 2005; Pokhrel et al. 2024) and can be described as a uniformly graded, medium sand with a minor content of silt (~2%). Tests for loosest and densest state were performed and revealed a maximum and minimum void ratio e of 0.980 and 0.621, respectively. The maximum porosity n_{max} results in 0.495 and the minimum n_{min} in 0.383.

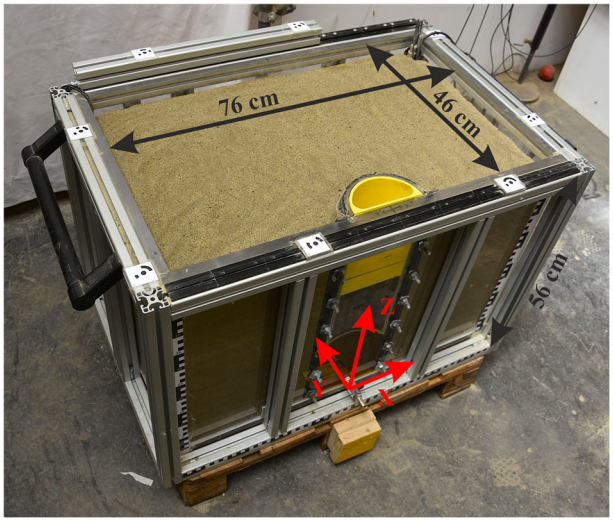

Figure 1. Test box before the test (perspective view).

To achieve the installation of the soil in the loosest possible manner while ensuring it is as fully saturated as feasible below the water table, a method akin to that of Yegian et al. (2007) was employed. The soil was installed in 14 layers, whereas for each layer the box was filled with water for three to four centimetres followed by the dry sand being rained into the water from just above the water table with a container, consisting of two layers of sieves. In Figure 2 it can be seen, that even though the soil was uniformly graded and the dropping heights of the grains were kept small, a slight stratification due to sedimentation during the installation can be observed.

In the centre of the front glass wall of the box, a perforated metal pipe with a semi-circular profile is located. Inside this metal pipe, an acrylic glass (transparent) and a 3D-printed inlay (yellow) seals the perforation so that only the lower 14 cm, depicted with (a) in Figure 2, are actually perforated and thus have a direct connection to the surrounding water. On the outer surface of the perforated metal profile, a filter fleece was placed to assure that no sand is getting inside the pipe.

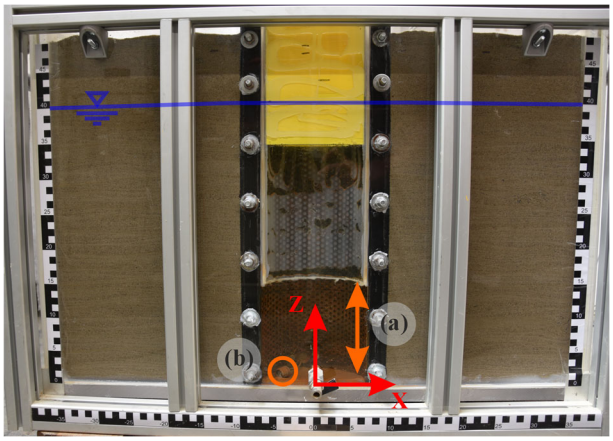

Figure 2. Test box before the test (front view).

The impulses are applied by means of a pneumatic cylinder to which a stamp was mounted that is travelling inside the 3D-printed inlay. On the outer perimeter of the stamp, a sealing ring was attached to get an almost tight system.

2.3 *Measurement devices*

Multiple measurement devices were used to investigate the pore pressure development and displacements resulting from the impulses. The former was measured by means of four miniature pore pressure transducers, containing a high-sensitivity piezoresistive chip, with a sample rate of 9600 Hz. With these types of sensors, small pore pressures can be measured, however, they cannot measure suction. Nevertheless, at very small pore pressures with quick changes in the pressures, negative pores pressure (suction) might be calculated due to their calibration. The results should therefore be treated with care and, in case of very small pressures (0-0.1 bar), considered primarily as qualitative distributions rather than accurate quantitative values. One was installed at the bottom of the box, inside the semi-circular profile, as depicted in Figure 2, marked with (b). Two were placed at a height of Z = 9 cm, approximately 20 and 35 cm away from the center of the semi-circular profile, in line with the rear corner of the box (negative x-axis). The remaining one is located at a height of Z = 22 cm, with a distance of 13 cm to the center of the semi-circular profile, in line to the rear corner on the positive x-axis. At the same height as the second level of pore pressure sensors, an accelerometer was installed on the positive x-axis, in line to the rear corner with a distance of app. 28 cm to the center, recording accelerations in three directions with a rate of app. 1540 Hz.

Surface settlements were measured using photogrammetry, for which eight markers were placed at the frame of the test box, as reference and control points. In total, 25 pictures of the surface were taken before and after the test, respectively, with the postprocessing being done in Agisoft Metashape (AgiSoft LLC).

To investigate the processes during the impulses also over depth, a Particle Image Velocimetry (PIV) camera was placed in front of the test box, capturing the full visible area of the axisymmetric. The camera, an Allied Vision Prosilica GX1920 mono, traces the moving sand particles and thus enables an evaluation of relative settlements over depth inside the box. This technique is usually used e.g. in hydraulic engineering, but has also been applied in geotechnical cases, see Krammer (2020). For the evaluation of the PIV-images, the open source software PIV-lab, developed by Thielicke and Sonntag (2021), was used. In combination with the photogrammetry, realistic 3D-settlements of the sand can be measured.

2.4 *Test execution*

After finishing the installation of the soil and the measurement devices, the box was left untouched and protected from unwanted vibrations for 48 hours before the test started.

Figure 3 shows the laboratory test setup, consisting of (1) the test box, (2) the surge trigger device, (3) the computer to control the frequency of the surges and record accelerations, (4) the equipment to record the pore pressures and (5) the PIV-camera. The surge trigger system is mounted on two blue beams supported by trestle legs and securely clamped in place using screw clamps. There is no physical connection between the surge trigger device and the test box except for the stamp to avoid vibrations being transferred to the box.

After positioning the stamp in the 3D-printed half-cylinder and adjusting the measuring devices, the surges were applied to the water in the semicircular profile at a frequency of 2.5 Hz for 31 seconds resulting in 78 impulses.

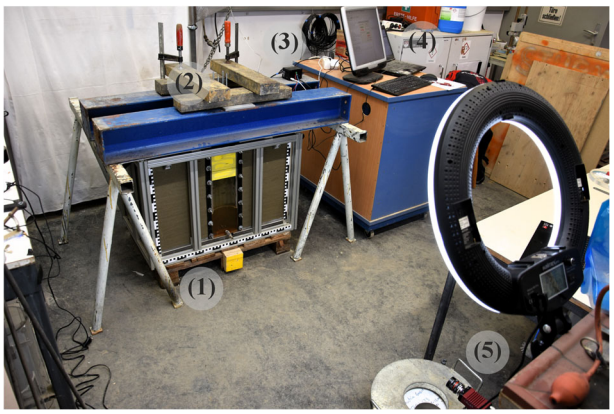

Figure 3. Laboratory test setup.

3 RESULTS AND DISCUSSION

Comparing the photogrammetry of the surface before and after the test it became visible that settlements in the magnitude of 10 to 30 mm occurred at the surface, depicted in Figure 4. It also shows, that settlements at the borders and corners are smaller and their maximum is more concentrated to the center of the box. The light areas in the back corners of the box show the data cables of the pore pressure transducers and therefore no settlements.

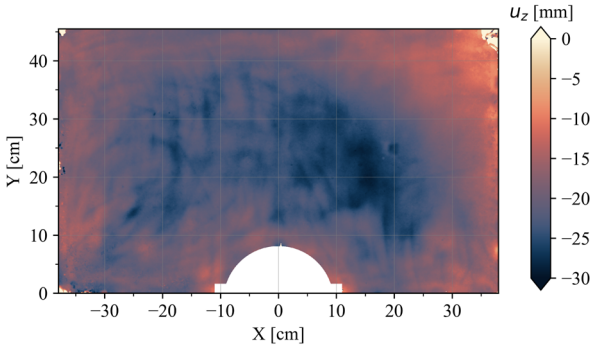

Figure 4. Total settlements (top view).

In total, the surface settled by 20 mm from a mean height of Z = 50 cm before the surges and Z = 48 cm after, which leads to overall relative settlements of 4%. Assuming an average initial density index $I_{D,init}$ of app. 30% after installation and before the surges, which corresponds to a loose state, the initial void ratio e_{init} was calculated with 0.872, according to Equation (1).

$$I_D = \frac{e_{max} - e}{e_{max} - e_{min}} \quad (1)$$

By using the relative settlements ε of 4%, the void ratio after the impulses e_{dens} can be calculate as shown in Equation (2) and results in 0.797. This leads to a relative density $I_{D,dens}$ of 51%, corresponding to a medium dense state.

$$e_{dens} = e_{init} - \varepsilon \cdot (1 + e_{init}) \quad (2)$$

During the execution of the test, movements of the particles became visible, due to a high hydraulic gradient between the inside of the pipe and the surrounding water in the soil. This can also be observed in the evaluation of the PIV-data in Figure 5, which shows the plot of the relative displacements. There, settlements are defined by negative values and heave by positive ones. In such hydraulic processes, the traced soil particles are moving with the stream of the ground water, thus showing large displacements. Due to such hydraulic effects, especially, both settlement and heave movements can be observed very close to one another as some particles are moving towards the surface and some are moving further down. In Figure 4 these effects are visible from a height of Z at app. 12 cm and upwards.

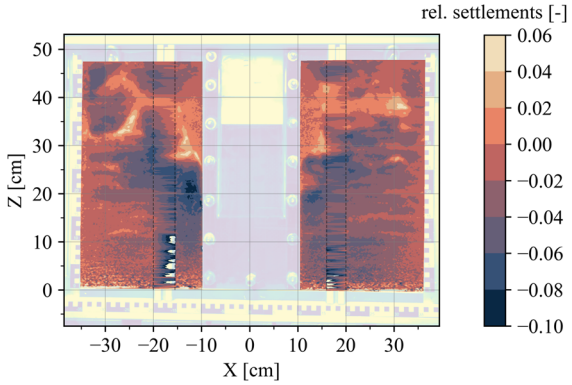

Figure 5. Relative settlements (front view).

In the area of the perforated part of the semi-circular profile, from the bottom to Z = 14 cm, almost constant relative settlements can be seen with a magnitude of roughly five percent on the right half along the positive x-axis and three to four on the left side. Similar to Figure 4 it can also be seen, that the right half has slight larger settlements compared to the left half. Close to the walls, the relative settlements seem to be influence by boundary effects and show smaller values. It should be noted, that the relative settlements of the invisible areas of the front acrylic glass, behind the metal frames, were interpolated.

The development of the pore pressure during the first four impulses is shown in Figure 6. From 0.00 s until the start of the first impulse at app. 1.30 s, the hydrostatic pore pressures are measured at each level of installment. In the center of the semi-circular profile at Z = 0 cm (level 1), P1 is located, showing the highest hydrostatic pore pressure, followed by P2 and P3 at Z = 9 cm (level 2) and P4 at Z = 22 cm (level 3). The continuous lines of P2 and P4 show the pore pressure transducers that were placed close to the perforated profile.

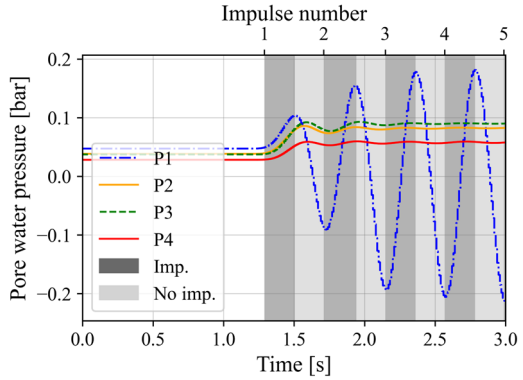

Figure 6. Pore pressure during the first four impulses.

Dark grey areas indicate triggered impulses, with their consecutive numbering shown on the upper x-axis of Figure 6, while light grey areas indicate an impulse release. Sensor P1 shows high changes in pore pressure with each single impulse, even reaching negative values, which cannot be measured with these type of sensors as explained in chapter 2.3. Sensors P2, P3 and P4 also show a significant increase at the first impulse and then remain at a rather constant level over the following three impulses. After about ten impulses, not shown in Figure 6,

a decrease of the measured pore pressures in P2, P3 and P4 starts and a change in the PW-pressures with each impulse is visible. Furthermore, it can be observed, that the peak in pore pressure of these three sensors is reached with a slight delay compared to P1 inside the perforated profile. During the first two impulses, small changes are measured, followed by almost no change in pore pressure starting with the third impulse.

4 CONCLUSIONS

With the novel soil improvement technique DYWIC, the risk of soil liquefaction can be reduced. This innovative method, which uses groundwater as a densification medium, was investigated under controlled laboratory conditions using multiple small-scale test boxes. The primary aims were to better understand soil behavior during impulse application and to evaluate the method's effectiveness.

The results indicate that the technique achieves measurable soil densification. Significant surface deformations and a distinct increase in the density index I_D were quantified through photogrammetry, while the PIV captured movement across the full depth along the axis of symmetry. Although sensitive to calibration, pore pressure transducers recorded a significant rise in pore pressure during impulse application, confirming the intended temporary reduction in effective stress.

Observations along the axis of symmetry provided valuable insight into depth-related effects; however, the semi-circular cylinder geometry presented sealing challenges at the stamp. Limitations associated with the test box dimensions-such as boundary effects and low stress levels-were unavoidable. Larger laboratory experiments, and ideally full-scale field trials, are needed to address these constraints. Field testing would enable evaluation under realistic stress conditions, facilitate assessment of the spatial extent of densification, and supply critical data for refining the technique toward practical application.

In summary, this initial laboratory study supports the feasibility of DYWIC as an innovative method for liquefaction mitigation. With further development and validation at larger scales, it could become a valuable addition to geotechnical engineering practice.

5 REFERENCES

AgiSoft LLC: Agisoft Metashape Professional. Version 2.1.3. 3D modeling from images and laser scans. Available online at www.agisoft.com.

Bao, Xiaohua; Jin, Zhiyang; Cui, Hongzhi; Chen, Xiangsheng; Xie, Xiongyao (2019): Soil liquefaction mitigation in geotechnical engineering: An overview of recently developed methods. In *Soil Dynamics and Earthquake Engineering* 120, pp. 273–291. DOI: 10.1016/j.soildyn.2019.01.020.

Huang, Yu; Wen, Zhuoqiang (2015): Recent developments of soil improvement methods for seismic liquefaction mitigation. In *Nat Hazards* 76 (3), pp. 1927–1938. DOI: 10.1007/s11069-014-1558-9.

Jefferies, Mike; Been, Ken (2016): Soil liquefaction. A critical state approach. Second edition. Boca Raton, London: CRC Press (Applied geotechnics series). Available online at https://www.taylorfrancis.com/books/9781482213676.

Kramer, Steven L.; Stewart, Jonathan P. (2025): Geotechnical earthquake engineering. Second edition. Boca Raton, London, New York: CRC Press Taylor & Francis Group.

Krammer, Christopher (2020): „Mud-Pumping" im Eisenbahnbau: Labortechnische Untersuchungen der Trennstabilität zwischen Unterböden aus Schluff-Sand-Gemischen und Gleisschotter unter dynamischen Vertikallasten. PhD-Thesis. Graz University of Technology, Graz, Austria. Institute of Soil Mechanics, Foundation Engineering and Computational Geotechnics.

Laue, Jan; Buchheister, J. (2005): Load path and loading velocity as potential condition indicator for liquefaction of silty soils. In : Proceedings of the 16th International Conference on Soil Mechanics and Geotechnical Engineering. International Conference on Soil Mechanics and Geotechnical Engineering: Geotechnology in Harmony with the Global Environment : 12/09/2005 - 16/09/2005. Rotterdam: Millpress (4), pp. 2677–2680. Available online at https://www.diva-portal.org/smash/record.jsf?pid=diva2:1000793, checked on 9/30/2016.

Mitchell, James K. (2012, c2008): Mitigation of Liquefaction Potential of Silty Sands. In James E. Laier, David K. Crapps, Mohamad H. Hussein (Eds.): From Research to Practice in Geotechnical Engineering. Symposium Honoring Dr. John H. Schmertmann for His Contributions to Civil Engineering at Research to Practice in Geotechnical Engineering Congress 2008. New Orleans, Louisiana, United States, March 9-12, 2008. Reston, VA: American Society of Civil Engineers (Geotechnical Special Publication, 180), pp. 433–451.

Pecker, Alain (2021): The H2020 European Project LiqueFACT. In *Bull Earthquake Eng* 19 (10), pp. 3803–3806. DOI: 10.1007/s10518-021-01168-z.

Pokhrel, Abilash; Chiaro, Gabriele; Kiyota, Takashi; Cubrinovski, Misko (2024): Liquefaction characteristics of sand-gravel mixtures: Experimental observations and its assessment based on intergranular state concept. In *Soils and Foundations* 64 (2).

Thielicke, William; Sonntag, René (2021): Particle Image Velocimetry for MATLAB: Accuracy and enhanced algorithms in PIVlab. In *JORS* 9 (1), p. 12. DOI: 10.5334/jors.334.

Yegian, M. K.; Eseller-Bayat, E.; Alshawabkeh, A.; Ali, S. (2007): Induced-Partial Saturation for Liquefaction Mitigation: Experimental Investigation. In *J. Geotech. Geoenviron. Eng.* 133 (4), pp. 372–380. DOI: 10.1061/(ASCE)1090-0241(2007)133:4(372).